Organometallics 1991, *10*, 2191-2198

(common to both complexes **13** and **14**) was idealized to C_s symmetry. Each of the HCCH and $HCPMe_2$ ligands was rotated through α°, about the *x* axis, which passes through the metal atom and the C–C, or P–C bond, so as to maintain constant Nb–C, or Nb–P, distances. For $\alpha = 0°$, the acetylene or phosphaacetylene ligand lies parallel to the C_5Me_5 ring. Thus, in **13**, $\alpha = 0°$, while, in **14**, $\alpha = +90°$. The role of the phosphorus 3d orbitals was tested by comparing the results of calculations in which the atomic orbital basis set of the P atom was restricted to valence 3s and 3p and then was expanded to include 3d orbitals.

The Fenske–Hall calculations employed single-ζ Slater functions for the 1s and 2s functions of C, P, and Cl. The exponents were obtained by curve fitting the double-ζ functions of Clementi[20] while orthogonal functions were maintained; the double-ζ functions were used directly for the 2p orbitals. For P, an expanded atomic orbital basis set used an exponent for the 3d functions of 1.80. An exponent of 1.16 was used for hydrogen. The Nb functions,[21] chosen for the +1 oxidation state, were augmented by 5s and 5p functions with exponents of 2.20.

Acknowledgment. V.C.G. wishes to thank the SERC for a research grant and a studentship (to T.P.K.). C.E.H. gratefully acknowledges the award of a 1983 University Research Fellowship by the Royal Society. H.M.A. thanks the laboratory of the Government Chemist for undergraduate sponsorship. We are also grateful to Dr. D. Reed for advice and help with high-field NMR experiments.

---

[20] Clementi, E. *J. Chem. Phys.* **1964**, *40*, 1944.

[21] Richardson, J. W.; Blackman, M. J.; Ranochak, J. E. *J. Chem. Phys.* **1973**, *58*, 3010.

1-Sila-3-metallacyclobutanes, Precursors for the Generation of Highly Electrophilic Group 4 Metallocene Alkyl Cations. Spectroscopic and Structural Evidence of a Weakly Bound THF Ligand in $[(C_5Me_5)_2Zr(CH_2SiMe_3)(THF)][BPh_4]$

David M. Amorose, Rip A. Lee, and Jeffrey L. Petersen*

Department of Chemistry, West Virginia University, Morgantown, West Virginia 26506-6045

Received December 7, 1990

The protonation of $L_n\overline{M(CH_2SiMe_2CH_2)}$ ($L_n = (C_5H_5)_2$, $SiMe_2(C_5H_4)_2$ M = Ti, Zr; $L_n = (C_5Me_5)_2$ M = Zr) with $[NEt_3H][BPh_4]$ in THF produces the corresponding (trimethylsilyl)methyl-substituted metal alkyl tetraphenylborate salts $[L_nM(CH_2SiMe_3)(THF)][BPh_4]$ (**1**–**5**). These complexes have been characterized by elemental analysis and ^1H and ^{13}C NMR measurements. The molecular structure of $[Cp^*_2Zr(CH_2SiMe_3)(THF)][BPh_4]$ (**5**) has been determined by X-ray diffraction methods. Complex **5** crystallizes in space group $P2_1/a$ with $a = 26.911$ (9) Å, $b = 13.929$ (4) Å, $c = 12.569$ (4) Å, $\beta = 101.73$ (2)°, $V = 4613$ (3) Å^3, and $Z = 4$. The steric bulk of the pentamethylcyclopentadienyl ligands controls the orientation of the THF molecule, placing it nearly "parallel" to the equatorial plane of the metallocene wedge. Attempts to prepare the THF-free cation $[Cp^*_2Zr(CH_2SiMe_3)]^+$ by the reaction of $Cp^*_2\overline{Zr(CH_2SiMe_2CH_2)}$ with $[N(n\text{-butyl})_3H][BPh_4]$ in toluene led to the isolation of the previously reported zwitterion $Cp^*_2Zr(+)\text{-}(m\text{-}C_6H_4)\text{-}B(-)Ph_3$ (**6**). Compounds **1**–**4** (in CH_2Cl_2) and compound **6** (in toluene) behave as ethylene polymerization catalysts, producing high-density polyethylene (HDPE) under mild conditions in the absence of an Al cocatalyst.

Introduction

Bis(cyclopentadienyl)metal complexes such as Cp_2MCl_2 (M = Ti, Zr) in the presence of aluminum alkyl reagents constitute an important class of soluble catalysts for Ziegler–Natta olefin polymerization.[1] Although initial efforts by Shilov and co-workers[2] to identify the catalytically active species were unsuccessful, they suggested that the polymerization process involves the participation of a highly electrophilic, cationic metallocene alkyl complex, Cp_2MR^+. Indirect evidence of its existence was provided by Eisch and co-workers,[3] who trapped and structurally characterized the cationic alkenyl species $[Cp_2Ti(C(SiMe_3){=}C(Ph)Me)][AlCl_4]$, following the addition of $PhC{\equiv}CSiMe_3$ to an active catalyst mixture containing titanocene dichloride and $AlMeCl_2$. Although the isolation of Cp_2TiMe^+ and related d^0, 14e$^-$ cations remains to be accomplished, several different synthetic strategies have been employed to prepare THF adducts of these species. Taube and Krukowka[4] have reported that $[Cp_2TiMe(THF)][BPh_4]$ is obtained by partial protonolysis of Cp_2TiMe_2 by $[NPhMe_2H][BPh_4]$ in a CH_2Cl_2/THF mixture. Similar strategies were employed by Marks and co-workers[5] to prepare a variety of cationic organothorium compounds, including $[Cp^*_2ThMe(THF)_2][BPh_4]$, and by Teuben and co-workers[6] for the preparation of $[Cp^*_2MMe(THT)][BPh_4]$, where M = Ti, Zr, Hf and THT

---

[1] (a) Natta, G.; Pino, P.; Mazzanti, G.; Giannini, U. *J. Inorg. Nucl. Chem.* **1958**, *18*, 612. (b) Breslow, D. S.; Newburg, N. R. *J. Am. Chem. Soc.* **1959**, *81*, 81. (c) Ziegler, K.; Gellert, H. G.; Zosel, K.; Holzkamp, E.; Schneider, J.; Soll, M.; Kroll, W. R. *Justus Liebigs Ann. Chem.* **1960**, *629*, 121. (d) Sinn, H.; Kolk, E. *J. Organomet. Chem.* **1966**, *6*, 373. (e) Sinn, H.; Kaminsky, W. *Adv. Organomet. Chem.* **1980**, *18*, 99.

[2] Dyachkovskii, F. S.; Shilova, A. K.; Shilov, A. E. *J. Polym. Sci., Part C* **1967**, *16*, 2333.

[3] Eisch, J. J.; Piotrowski, A. M.; Brownstein, S. K.; Gabe, E. J.; Lee, F. L. *J. Am. Chem. Soc.* **1985**, *107*, 7219.

[4] Taube, R.; Krukowka, L. *J. Organomet. Chem.* **1988**, *C9*, 347.

[5] Lin, Z.; Le Marechal, J.-F.; Sabat, M.; Marks, T. J. *J. Am. Chem. Soc.* **1987**, *109*, 4127.

[6] Eshuis, J. J. W.; Tan, Y. Y.; Teuben, J. H.; Renkema, J. *J. Mol. Catal.* **1990**, *62*, 277.

0276-7333/91/2310-2191$02.50/0

is tetrahydrothiophene. Bochmann and co-workers[7] have prepared $[Cp^*_2TiMe(THF)][BPh_4]$ by the oxidation of Cp^*_2TiMe with $AgBPh_4$ in THF. Jordan and co-workers[8] have relied on the one-electron oxidation of a neutral zirconocene dialkyl complex with either $AgBPh_4$ in CH_3CN or $[Cp_2Fe][BPh_4]$ in THF to prepare a series of zirconocene alkyl cations, $[Cp_2ZrR(L)]^+$ (R = Me, Ph, CH_2Ph; L = CH_3CN, THF). Reactivity studies[9] have shown that $[Cp_2ZrR(THF)]^+$ catalyzes the polymerization of ethylene in the absence of Al cocatalysts or oxide supports.

During preliminary investigations of the reactivity of $Cp_2Zr(CH_2SiMe_2CH_2)$, we[10] observed that its reaction with phenylacetylene proceeds with the formation of the acetylide complex $Cp_2Zr(C{\equiv}CPh)(CH_2SiMe_3)$. This result suggested that protonation of a 1-sila-3-metallacyclobutane ring with a weak acid containing a sterically crowded or poorly donating conjugate base will not only open a metal coordination site but may also provide a convenient method for generating the corresponding metallocene–(trimethylsilyl)methyl cation. To explore the general applicability of this approach, we have reacted $[NEt_3H][BPh_4]$ with several group 4 1-sila-3-metallacyclobutane complexes, including $Cp_2M(CH_2SiMe_2CH_2)$ (M = Ti, Zr),[11] $[SiMe_2(C_5H_4)_2]M(CH_2SiMe_2CH_2)$ (M = Ti, Zr),[12] and $Cp^*_2Zr(CH_2SiMe_2CH_2)$.[13] The resultant cationic species have been characterized in solution by ^1H and ^{13}C NMR measurements, and the molecular structure of $[Cp^*_2Zr(CH_2SiMe_3)(THF)][BPh_4]$ has been determined by X-ray diffraction methods. Further details regarding the characterization of these cations and their catalytic activity toward ethylene polymerization are described herein.

Experimental Section

Reagents. All hydrocarbon and ethereal solvents (reagent grade) were purified by standard techniques[14] and vacuum-distilled from storage flasks containing $[Cp_2Ti(\mu\text{-}Cl)_2]_2Zn$.[15] Methylene chloride was distilled from P_4O_{10}. Hydrobromic acid (48%; Fisher); triethylamine (Aldrich), sodium tetraphenylborate (Boulder Scientific), and *n*-butyllithium (Aldrich) were used as received. Tributylamine (Aldrich) was dried over 4A molecular sieves and stored under nitrogen. Gaseous HCl was dried by passing through $CaSO_4$. Deuterated solvents (Aldrich or Cambridge Isotopes) were vacuum-distilled from 4A molecular sieves. $Cp_2M(CH_2SiMe_2CH_2)$ (M = Ti, Zr),[11] $[SiMe_2(C_5H_4)_2]M(CH_2SiMe_2CH_2)$ (M = Ti, Zr),[12] $Cp^*_2Zr(CH_2SiMe_2CH_2)$,[13] and $Cp^*_2ZrMe_2$[16] were prepared by using published procedures.

Elemental Analyses. Elemental analyses were carried out by Dornis and Kolbe Microanalytical Laboratory, Mülheim a. d. Ruhr, Germany (DK), or by Oneida Research Services, Inc., Whitesboro, NY (ORS).

Instrumentation. ^1H and ^{13}C NMR spectra were recorded with a JEOL GX-270 FT-NMR spectrometer operating in the FT mode at 270 MHz (^1H) or 67.5 MHz (^{13}C). The ^1H chemical shifts are referenced to the residual proton peak of $CH_2Cl_2\text{-}d_2$ at 5.32 ppm (vs TMS), to the residual proton peak of acetone-d_6 at 2.04 ppm (vs TMS), to the residual methyl proton peak of toluene-d_8 at 2.09 ppm (vs TMS), or to the residual α-CH_2 proton peak of THF-d_8 at 3.58 pm (vs TMS). The ^{13}C resonances are referenced to the central peak of $CH_2Cl_2\text{-}d_2$ at δ 53.8 (vs TMS), to the central peak of acetone-d_6 at δ 29.8 (vs TMS), or to the central α-C resonance of THF-d_8 centered at 67.4 (vs TMS).

Infrared spectra were measured on a Perkin-Elmer 1310 IR spectrometer or a Perkin-Elmer 1600 series FT-IR spectrometer using KBr disks. Melting point measurements were carried out with the aid of a Laboratory Devices Mel-Temp apparatus. Electronic spectra were recorded on a Hewlett-Packard HP8452A diode array spectrometer using a 1.00-cm quartz cell equipped with a Teflon stopcock.

General Procedures. All reactions and manipulations were carried out on a double-manifold, high-vacuum line or in a Vacuum Atmospheres glovebox. Nitrogen and argon were prepurified by passage over reduced BTS catalysts and 4A molecular sieves. All glassware was thoroughly oven-dried and/or flame-dried under vacuum prior to use. Stoichiometric amounts of volatile reagents were added to a reaction mixture by condensation from a calibrated gas bulb. Small-scale ethylene polymerization experiments were performed in either 10-mm thick-walled glass tubes or medium-wall NMR tubes.

Synthesis of Trialkylammonium Salts. The trialkylammonium salts $[NEt_3H][BPh_4]$ and $[N(n\text{-butyl})_3H][BPh_4]$ were prepared by following the procedures originally developed by Wittig and co-workers.[17] Equimolar amounts of the trialkylammonium halide salt (NEt_3HBr or $N(n\text{-butyl})_3HCl$) and $NaBPh_4$ were dissolved in a minimum amount of distilled water and mixed by slow addition of the latter with vigorous stirring. The resultant white precipitate was collected by filtration, washed with water, and dried under vacuum. Recrystallization of $[NEt_3H][BPh_4]$ from a 3:1 methanol/acetone solution and of $[N(n\text{-butyl})_3H][BPh_4]$ from acetone gave suitable crystalline samples of these salts in good yield.

$[NEt_3H][BPh_4]$. ^1H NMR spectrum (acetone-d_6): δ 7.33 (m, *o* CH), 6.93 (t, *m* CH, $^3J_{H-H}$ = 7.1 Hz), 6.78 (t, *p* CH, $^3J_{H-H}$ = 7.1 Hz), 3.36 (q, CH_2, $^3J_{H-H}$ = 7.3 Hz), 1.33 (t, CH_3, $^3J_{H-H}$ = 7.3 Hz). Gated nondecoupled ^{13}C NMR spectrum (acetone-d_6): δ 164.1 (q, C_{ipso}, $^1J_{C-B}$ = 49 Hz), 136.9 (d, *m* CH, $^1J_{C-H}$ = 154 Hz), 125.9 (d, *o* CH, $^1J_{C-H}$ = 151 Hz), 122.1 (d, *p* CH, $^1J_{C-H}$ = 155 Hz), 48.1 (t, CH_2, $^1J_{C-H}$ = 143 Hz), 9.3 (q, CH_3, $^1J_{C-H}$ = 128 Hz).

$[N(n\text{-butyl})_3H][BPh_4]$. ^1H NMR spectrum (acetone-d_6): δ 7.33 (m, *o* CH), 6.93 (t, *m* CH, $^3J_{H-H}$ = 7.1 Hz), 6.78 (t, *p* CH, $^3J_{H-H}$ = 7.1 Hz), 3.26 (m, NCH_2), 1.87–1.75 (m, CH_2CH_3), 1.40 (m, NCH_2CH_2), 0.94 (t, CH_3, $^3J_{H-H}$ = 7.3 Hz). $^{13}C\{^1H\}$ NMR spectrum (acetone-d_6): δ 164.5 (q, C_{ipso}, $^1J_{C-B}$ = 49 Hz), 137.0 (*m* CH), 125.9 (*o* CH), 122.2 (*p* CH), 53.9 (NCH_2), 26.3 (CH_2CH_3), 20.5 (NCH_2CH_2), 13.8 (CH_3).

Synthesis of Metallocene (Trimethylsilyl)methyl Cations. The same general procedure was used for the preparation of $[Cp_2M(CH_2SiMe_3)(THF)][BPh_4]$ (M = Ti (**1**), Zr (**2**)), $\{[SiMe_2(C_5H_4)_2]M(CH_2SiMe_3)(THF)\}[BPh_4]$ (M = Ti (**3**), Zr (**4**)), and $[Cp^*_2Zr(CH_2SiMe_3)(THF)][BPh_4]$ (**5**). A general procedure is described below for the preparation of $[Cp_2Ti(CH_2SiMe_3)(THF)][BPh_4]$ with pertinent information provided separately for the other compounds.

$[Cp_2Ti(CH_2SiMe_3)(THF)][BPh_4]$ (1). In a typical reaction, 0.556 g (1.32 mmol) of $[NEt_3H][BPh_4]$ and 0.407 g (1.54 mmol, 17% excess) of $Cp_2Ti(CH_2SiMe_2CH_2)$ were added to a 100-mL Solv-seal flask attached to a pressure-equalizing filter frit and the flask was then evacuated. Approximately 35 mL of THF was condensed in the flask via vacuum distillation, and the solution was stirred at 25 °C for 2–3 h. THF was then removed in vacuo, and the residue was washed twice with 20-mL aliquots of pentane to remove triethylamine and unreacted metallacycle, once with cold methylene chloride (kept at −70 °C for 1 h), and a final time with pentane. The finely divided, pale orange product was dried

---

(7) Bochmann, M.; Jagger, A. J.; Wilson, L. M.; Hursthouse, M. B.; Motevalli, M. *Polyhedron* **1989**, *8*, 1838.

(8) (a) Jordan, R. F.; Dasher, W. E.; Echols, S. F. *J. Am. Chem. Soc.* **1986**, *108*, 1718. (b) Jordan, R. F.; LaPointe, R. E.; Bajgur, C. S.; Echols, S. F.; Willett, R. *J. Am. Chem. Soc.* **1987**, *109*, 4111.

(9) (a) Jordan, R. F. *J. Chem. Educ.* **1988**, *65*, 285. (b) Jordan, R. F.; Bradley, P. K.; LaPointe, R. E.; Taylor, D. F. *New J. Chem.* **1990**, *14*, 505.

(10) Tikkanen, W. R.; Petersen, J. L., unpublished results.

(11) Tikkanen, W. R.; Liu, J. Z.; Egan, J. W., Jr.; Petersen, J. L. *Organometallics* **1984**, *3*, 825.

(12) Kabi-Satpathy, A.; Bajgur, C. S.; Reddy, K. P.; Petersen, J. L. *J. Organomet. Chem.* **1989**, *364*, 105.

(13) Petersen, J. L.; Egan, J. W., Jr. *Organometallics* **1987**, *6*, 2007.

(14) Gordon, A. J.; Ford, R. A. *The Chemist's Companion*; Wiley-Interscience: New York, 1972; pp 431–436.

(15) Sekutowski, D. G.; Stucky, G. D. *Inorg. Chem.* **1975**, *14*, 2192.

(16) Manriquez, J. M.; McAlister, D. R.; Sanner, R. D.; Bercaw, J. E. *J. Am. Chem. Soc.* **1978**, *100*, 2716.

(17) (a) Wittig, G.; Raff, P. *Justus Liebigs Ann. Chem.* **1951**, *573*, 195. (b) Wittig, G.; Keicher, G.; Rückert, A.; Raff, P. *Justus Liebigs Ann. Chem.* **1949**, *563*, 110. (c) Wittig, G.; Herwig, W. *Chem. Ber.* **1955**, *88*, 962.

in vacuo (yield 59%). Anal. Calcd for $C_{42}H_{49}BOSiTi$: C, 76.82; H, 7.52. Found: C, 76.84; H, 7.51; N, 0.0 (ORS). ^{1}H NMR spectrum (CD_2Cl_2): δ 7.36 (m, *o* CH), 7.06 (t, *m* CH, $^3J_{H-H}$ = 7.3 Hz), 6.91 (t, *p* CH, $^3J_{H-H}$ = 7.0 Hz), 6.34 (s, C_5H_5), 3.41 (s, $TiCH_2$), 3.03 (m, α-CH_2 (THF)), 1.71 (m, β-CH_2 (THF)), 0.09 (s, $SiMe_3$). $^{13}C\{^1H\}$ NMR spectrum (CD_2Cl_2): δ 164.4 (q, C_{ipso}, $^1J_{C-B}$ = 49 Hz), 136.3 (*m* CH), 126.1 (*o* CH), 122.2 (*p* CH), 118.1 (C_5H_5), 110.0 ($TiCH_2$), 77.3 (α-CH_2 (THF)), 25.7 (β-CH_2 (THF)), 2.9 ($SiMe_3$).

[$Cp_2Zr(CH_2SiMe_3)(THF)$][BPh_4] (2). With molar amounts similar to those used in the preparation of **1**, a pale yellow powder of **2** was collected in 48% overall yield. Anal. Calcd for $C_{42}H_{49}BOSiZr$: C, 72.07; H, 7.06. Found: C, 72.25; H, 6.96; N, 0.02 (ORS). ^{1}H NMR spectrum (CD_2Cl_2): δ 7.36 (m, *o* CH), 7.06 (t, *m* CH, $^3J_{H-H}$ = 7.3 Hz), 6.92 (t, *p* CH, $^3J_{H-H}$ = 7.1 Hz), 6.32 (s, C_5H_5), 3.34 (m, α-CH_2 (THF)), 1.77 (m, β-CH_2 (THF)), 1.67 (s, $ZrCH_2$), 0.12 (s, $SiMe_3$). $^{13}C\{^1H\}$ NMR spectrum (CD_2Cl_2): δ 164.4 (q, C_{ipso}, $^1J_{C-B}$ = 49 Hz), 136.3 (*m* CH), 126.2 (*o* CH), 122.2 (*p* CH), 114.7 (C_5H_5), 78.5 (α-CH_2 (THF)), 76.4 ($ZrCH_2$), 25.9 (β-CH_2 (THF)), 3.2 ($SiMe_3$).

{[$SiMe_2(C_5H_4)_2$]$Ti(CH_2SiMe_3)(THF)$}[BPh_4] (3). The cold methylene chloride wash was neglected because a clean ^{1}H NMR spectrum of **3** in CD_2Cl_2 was obtained after the initial pentane wash. A pale orange powder (yield 85%) was collected. Anal. Calcd for $C_{44}H_{53}Si_2BOTi$: C, 74.15; H, 8.06. Found: C, 73.83; H, 7.54 (DK). ^{1}H NMR spectrum (CD_2Cl_2): δ 7.37 (m, *o* CH), 7.07 (t, *m* CH, $^3J_{H-H}$ = 7.3 Hz), 6.93 (t, *p* CH, $^3J_{H-H}$ = 7.1 Hz), 7.85, 6.64, 5.88, 5.48 (m, C_5H_4), 3.39 (s, $TiCH_2$), 3.05 (m, α-CH_2 (THF)), 1.69 (m, β-CH_2 (THF)), 0.78, 0.55 (s, $SiMe_2$), 0.15 (s, $SiMe_3$). $^{13}C\{^1H\}$ NMR spectrum (CD_2Cl_2): δ 164.3 (q, C_{ipso}, $^1J_{C-B}$ = 49 Hz), 136.3 (*m* CH), 126.0 (*o* CH), 122.2 (*p* CH), 131.6, 129.3, 119.1, 117.2 (distal and proximal carbons of C_5H_4), 113.3 (bridgehead carbon of C_5H_4), 106.5 ($TiCH_2$), 77.6 (α-CH_2 (THF)), 25.6 (β-CH_2 (THF)), 2.8 ($SiMe_3$), −5.2, −5.9 ($SiMe_2$).

{[$SiMe_2(C_5H_4)_2$]$Zr(CH_2SiMe_3)(THF)$}[BPh_4] (4). The additional washing of the product with cold CH_2Cl_2 was not necessary because a clean ^{1}H NMR spectrum of **4** in CD_2Cl_2 was obtained after the first pentane wash. A pale yellow powder (yield 86%) was collected. Anal. Calcd for $C_{44}H_{53}Si_2BOZr$: C, 69.90; H, 7.06. Found: C, 69.88; H, 6.92; N, 0.07 (ORS). ^{1}H NMR spectrum (CD_2Cl_2): δ 7.36 (m, *o* CH), 7.07 (t, *m* CH, $^3J_{H-H}$ = 7.3 Hz), 6.93 (t, *p* CH, $^3J_{H-H}$ = 7.1 Hz), 6.40, 5.98, 5.75 (m, C_5H_4[18]), 3.43 (m, α-CH_2 (THF)), 1.78 (m, β-CH_2 (THF)), 1.52 (s, $ZrCH_2$), 0.79, 0.63 (s, $SiMe_2$), 0.14 (s, $SiMe_3$). $^{13}C\{^1H\}$ NMR spectrum (CD_2Cl_2): δ 164.4 (q, C_{ipso}, $^1J_{C-B}$ = 49 Hz), 136.3 (*m* CH), 126.1 (*o* CH), 122.2 (*p* CH), 131.6, 127.7, 122.7, 116.5, 114.3 (bridgehead, proximal, and distal carbons of C_5H_4), 79.2 ($ZrCH_2$), 78.5 (α-CH_2 (THF)), 25.9 (β-CH_2 (THF)), 2.9 ($SiMe_3$), −5.0, −5.5 ($SiMe_2$).

[$Cp^*_2Zr(CH_2SiMe_3)(THF)$][$BPh_4$] (5). After a THF solution of $Cp^*_2\overline{Zr(CH_2SiMe_2CH_2})$ and [NEt_3H][BPh_4] was stirred for 1 day, the volume of THF was reduced and the solid was washed with pentane (2 × 20 mL) and toluene (3 × 20 mL). The *pale* yellow residue was dried in vacuo. A preliminary ^{1}H NMR spectrum of the residue was measured immediately after a few milligrams of the residue was dissolved in toluene-d_8 and then monitored periodically over a period of several days. The initial spectrum revealed the presence of two different species, namely **5** and the "THF-free" cation, **5′**, in solution. The proton resonances of the Cp* and $SiMe_3$ groups of **5** are located at δ 1.81 and 0.005, respectively, whereas those for **5′** are found at δ 1.77 and 0.24, respectively. The relative intensity ratio of these two singlets is ca. 3:1 in each case, consistent with the presence of two Cp* ligands and a $SiMe_3$ group in both **5** and **5′**. Upon standing, the resonances of **5** and **5′** are replaced after 3 days by those of a new species, **5″**. At this point, the ^{1}H NMR spectrum exhibits a Cp* resonance at δ 1.81 with a relative intensity half of that observed in the original spectrum and a singlet at ca. δ 0.00 with a relative intensity 33% greater than that observed in the initial spectrum. Four distinct singlets initially appearing at δ 1.36, 1.69, 1.87, and 1.95 are gradually replaced by singlets of comparable intensity at δ 1.69, 1.85, 1.86, and 2.14. Although **5″** remains to be isolated and fully characterized, these dramatic changes in this ^{1}H NMR spectrum are consistent with reaction sequence 1 and are indicative of the relative ease with which THF can be displaced from

$$\begin{aligned}&\underset{\mathbf{5}}{[Cp^*_2Zr(CH_2SiMe_3)(THF)]^+} \rightleftarrows \underset{\mathbf{5'}}{[Cp^*_2Zr(CH_2SiMe_3)]^+} + \\ &\quad THF \rightarrow \underset{\mathbf{5''}}{[Cp^*(\eta^1,\eta^5\text{-}C_5Me_4CH_2)Zr(THF)]^+} + TMS \quad (1)\end{aligned}$$

5 to produce the "THF-free" cation **5′**. Under these conditions of low THF concentration, the electrophilic Zr center of **5′** is sufficiently reactive to activate intramolecularly a C–H bond of one of its Cp* rings,[19] thereby promoting the elimination of $SiMe_4$ and the concomitant formation of a metalated cyclopentadienyl cation, presumably [$Cp^*(\eta^1,\eta^5\text{-}C_5Me_4CH_2)Zr(THF)$]$^+$.

The equilibrium between **5** and **5′** in (1) has been further established by adding roughly a 10-fold excess of THF to another NMR tube containing a few milligrams of the initial product residue and toluene-d_8. Under these conditions, only resonances for **5** are observed within NMR detection limits. By shifting the equilibrium to favor the formation of **5**, the additional THF made it possible to assign a previously obscured proton resonance at δ 1.76 to the methylene group of **5**.

From these NMR experiments, successive washings of **5** with toluene (by removing THF from solution) clearly encourage the conversion of **5** to **5′**. To circumvent this problem, the initial product was redissolved in THF. The solvent was slowly removed into a liquid-N_2-filled trap, leaving a *bright* yellow solid, which was neither washed with toluene nor placed under high vacuum. Its proton NMR spectrum in toluene-d_8 contained only resonances for **5**. Due to its low solubility in toluene, the ^{13}C NMR spectrum of **5** was measured in THF-d_8 and indicated the presence of a detectable amount of [NEt_3H][BPh_4][20] in the product. Efforts to remove this impurity by solvent extraction methods are hindered by the similar solubility properties of **5** and [NEt_3H][BPh_4] in polar solvents and by the inherent tendency of **5** to lose THF in nonpolar solvents. This result explains why earlier elemental analyses performed on **5** revealed the presence of at least 0.3% N. ^{1}H NMR spectrum (toluene-d_8): δ 7.63, 7.25, 7.13 (m, *o* CH, *m* CH, and *p* CH of BPh_4^-), 3.56 (m, α-CH_2 (THF)), 1.81 (s, C_5Me_5), 1.76 (s, $ZrCH_2$), 1.45 (m, β-CH_2 (THF)), 0.005 (s, $SiMe_3$). ^{1}H NMR spectrum (THF-d_8): δ 7.26 (m, *o* CH), 6.85 (t, $^3J_{H-H}$ = 7.4 Hz, *m* CH), 6.71 (t, $^3J_{H-H}$ = 7.2 Hz, *p* CH), 3.58 (m, α-CH_2 (THF)), 1.93 (s, C_5Me_5), 1.88 (s, $ZrCH_2$), 1.73 (m, β-CH_2 (THF)), 0.21 (s, $SiMe_3$). Gated nondecoupled ^{13}C NMR spectrum (THF-d_8): δ 165.1 (q, $^1J_{C-B}$ = 49.7 Hz, C_{ipso}), 137.1 (d, $^1J_{C-H}$ = 153.8 Hz, *m* CH), 125.7 (d, $^1J_{C-H}$ = 151.4 Hz, *o* CH), 125.5 (s, C_5Me_5), 122.0 (d, $^1J_{C-H}$ = 155.1 Hz, *p* CH), 76.4 (t, $^1J_{C-H}$ = 100.1 Hz, $ZrCH_2$), 12.4 (q, $^1J_{C-H}$ = 127.3 Hz, $C_5\mathit{Me}_5$), 5.5 (q, $^1J_{C-H}$ = 118.0 Hz, $SiMe_3$).

Synthesis of $Cp^*_2Zr(+)$-(*m*-C_6H_4)-$B(-)Ph_3$ (6). A 0.992-g (1.96-mmol) sample of [N(*n*-butyl)$_3$H][BPh_4] and a 0.967-g (2.16-mmol) sample of $Cp^*_2\overline{Zr(CH_2SiMe_2CH_2})$ were added to a 100-mL Solv-seal flask attached to a pressure-equalizing frit, and the vessel was then evacuated. Toluene was added to the flask, and the solution was stirred at room temperature with the formation of an orange solid precipitate after 2 h. After removal of volatiles in vacuo, the residue was washed with pentane (2 × 40 mL) to remove any unreacted metallacycle and tributylamine. The pale orange solid was dried in vacuo to give 0.321 g of an orange product (yield 42%). This solid is only slightly soluble in toluene. Its infrared spectrum (KBr disk) and electronic spectrum (toluene) are identical with those of an authentic sample of $Cp^*_2Zr(+)$-(*m*-C_6H_4)-$B(-)Ph_3$ prepared by the reaction of $Cp^*_2ZrMe_2$ with [N(*n*-butyl)$_3$H][BPh_4].[21] A faint orange toluene solution of this zwitterion exhibits a distinct electronic absorption at 294 nm and a barely detectable broad band at 460 nm.

Anal. Calcd for $C_{44}H_{49}BZr$: C, 77.73; H, 7.26. Found: C, 78.03; H, 6.87; N, 0.06 (ORS).

---

(18) The fourth multiplet was not resolved due to peak overlap.

(19) (a) McDade, C.; Green, J. C.; Bercaw, J. E. *Organometallics* **1982**, *1*, 1629. (b) Bulls, A. R.; Schaefer, W. P.; Serfas, M.; Bercaw, J. E. *Organometallics* **1987**, *6*, 1219. (c) Parkin, G.; Bunel, E.; Burger, B. J.; Trimmer, M. S.; Van Asselt, A.; Bercaw, J. E. *J. Mol. Catal.* **1987**, *41*, 21. (d) Parkin, G.; Bercaw, J. E. *Organometallics* **1989**, *8*, 1172. (e) Schock, L. E.; Brock, C. P.; Marks, T. J. *Organometallics* **1987**, *6*, 232.

(20) The assignments of the resonances due to the [NEt_3H]$^+$ cation in the ^{13}C NMR spectrum of **5** in THF-d_8 were made by the comparison with the corresponding spectrum of [NEt_3H][BPh_4] in THF-d_8.

(21) Hlatky, G. G.; Turner, H. W.; Eckman, R. R. *J. Am. Chem. Soc.* **1989**, *111*, 2728.

Table I. Data for the X-ray Diffraction Analysis of $[Cp^*_2Zr(CH_2SiMe_3)(THF)][B(C_6H_5)_4]$

A. Crystal Data

cryst syst	monoclinic	V, Å^3	4613 (3)
space group	$P2_1/a$ (C_{2h}^5, No. 14)	fw	840.24
a, Å	26.911 (9)	d(calcd), g/cm^3	1.210
b, Å	13.929 (4)	Z	4
c, Å	12.569 (4)	μ, cm^{-1}	2.99
β, deg	101.73 (2)		

B. Data Collection and Analysis Summary

cryst dimens, mm	0.20 × 0.375 × 0.50
rflns sampled	$\pm h,k,l$ ($5° < 2\theta < 45°$)
2θ range for centered rflns, deg	$30 < 2\theta < 35$
scan rate, deg/min	2.5
scan width, deg	$1.1 + 0.8 \tan \theta$
no. of std rflns	3
cryst decay, %	4
total no. of measd rflns	6385
no. of unique data used	3608 ($F_o^2 > 3.0\sigma(F_o^2)$)
agreement between equiv data	
$R_{av}(F_o)$	0.023
$R_{av}(F_o^2)$	0.025
P	0.03
discrepancy indices	
$R(F_o)$	0.052
$R(F_o^2)$	0.062
$R_w(F_o^2)$	0.096
σ_1	1.81
no. of variables	513
data to param ratio	7.03:1

X-ray Data Collection. A suitable crystalline sample of $[Cp^*_2Zr(CH_2SiMe_3)(THF)][BPh_4]$ was obtained by controlling the rate of solvent diffusion from a saturated THF solution into a separate reservoir containing toluene. The crystal was wedged into a glass capillary that was sealed under a prepurified nitrogen atmosphere in a locally constructed drybox. The sample was optically aligned on a Picker goniostat under computer control by a Krisel Control diffractometer automation system. The orientation angles for several low-angle reflections were used by an automatic-indexing algorithm[22] to calculate initial unit cell parameters. The orientation angles of 20 higher-order reflections were then optimized by an automatic peak-centering routine[23] and least-squares fit to provide the refined lattice parameters and the orientation matrix. The systematic absences ($\{h0l\}$, $h = 2n + 1$; $\{0k0\}$, $k = 2n + 1$) are consistent with the space group $P2_1/a$.

Intensity data ($\pm h,k,l$) were measured with Zr-filtered Mo Kα X-ray radiation with a takeoff angle of 2°. Peak scans employing the θ–2θ mode were made with a fixed scan rate and a variable scan width. The integrated intensity, I, and its standard deviation, $\sigma_c(I)$, for each measured reflection were calculated from the equations $I = w(S/t_s - B/t_b)$ and $\sigma_c(I) = w(S/t_s^2 + B/t_b^2)$, where S is the total scan count in time t_s and B is the combined background count in time t_b. The standard deviation of the square of each structure factor, $F_o^2 = I/Lp$, was calculated from the expression $\sigma(F_o^2) = [\sigma_c(F_o^2)^2 + (PF_o^2)^2]^{1/2}$. Duplicate reflections were averaged. Pertinent crystallographic data are summarized in Table I.

Structural Solution and Refinement. Initial coordinates for Zr, Si, and several other non-hydrogen atoms of $[Cp^*_2Zr(CH_2SiMe_3)(THF)][BPh_4]$ were obtained from an interpolation of the E map calculated on the basis of the phases determined by MULTAN78.[24] The remaining non-hydrogen atoms were located by Fourier methods and refined with anisotropic thermal parameters. At this point in the refinement it became apparent that the thermal ellipsoids for C6 and C7 of the coordinated molecule of THF were highly anisotropic. Efforts to fit this feature to a 2-fold disorder, however, were unsuccessful. Initial positions for all of the hydrogen atoms (except those bonded to C6 or C7) were either calculated with use of MIRAGE[25] or obtained from difference Fourier syntheses computed with use of only low-angle data with $(\sin \theta)/\lambda < 0.40$ Å^{-1}. The positional parameters for all of the located hydrogen atoms were partially refined with the non-hydrogen atoms fixed. However, due to space limitations in the least-squares refinement program, only the positional parameters of the hydrogens (H1 and H2) of the methylene group bound to Zr were varied along with those of the non-hydrogen atoms during the final refinement. Full-matrix refinement (based on F_o^2)[26-30]

Table II. Positional Parameters for the Non-Hydrogen Atoms in $[Cp^*_2Zr(CH_2SiMe_3)(THF)][B(C_6H_5)_4]$[a]

atom	x	y	z
Zr	0.32688 (2)	0.26112 (3)	0.68047 (5)
Si	0.2563 (1)	0.2479 (1)	0.9311 (1)
O	0.4100 (1)	0.2642 (3)	0.7548 (3)
C1	0.3064 (2)	0.2546 (3)	0.8442 (5)
C2	0.1926 (2)	0.2053 (5)	0.8621 (6)
C3	0.2771 (3)	0.1670 (5)	1.0489 (6)
C4	0.2463 (3)	0.3675 (5)	0.9911 (6)
C5	0.4530 (2)	0.2509 (5)	0.7001 (6)
C6	0.5001 (3)	0.2670 (9)	0.7821 (7)
C7	0.4876 (3)	0.3002 (7)	0.8801 (7)
C8	0.4322 (3)	0.2834 (5)	0.8697 (6)
C9	0.3517 (3)	0.4343 (4)	0.6404 (7)
C10	0.3172 (3)	0.4430 (4)	0.7104 (6)
C11	0.2705 (3)	0.4089 (4)	0.6560 (7)
C12	0.2747 (3)	0.3801 (4)	0.5519 (6)
C13	0.3256 (3)	0.3937 (4)	0.5424 (6)
C14	0.3017 (3)	0.0864 (4)	0.6905 (6)
C15	0.3503 (3)	0.0837 (4)	0.6673 (6)
C16	0.3478 (3)	0.1219 (4)	0.5631 (7)
C17	0.2969 (4)	0.1467 (4)	0.5208 (7)
C18	0.2684 (2)	0.1262 (4)	0.6013 (7)
C19	0.4035 (3)	0.4771 (5)	0.6606 (7)
C20	0.3285 (3)	0.4938 (4)	0.8177 (6)
C21	0.2203 (2)	0.4155 (4)	0.6925 (6)
C22	0.2288 (3)	0.3667 (4)	0.4614 (6)
C23	0.3475 (3)	0.3858 (5)	0.4426 (6)
C24	0.2869 (3)	0.0343 (4)	0.7828 (6)
C25	0.3952 (3)	0.0358 (5)	0.7387 (6)
C26	0.3882 (3)	0.1178 (5)	0.4941 (6)
C27	0.2757 (3)	0.1652 (5)	0.4022 (7)
C28	0.2119 (3)	0.1296 (4)	0.5860 (6)
C29	0.5235 (2)	0.2673 (4)	0.3745 (5)
C30	0.5069 (2)	0.3428 (4)	0.4297 (5)
C31	0.5322 (3)	0.3730 (5)	0.5322 (6)
C32	0.5755 (3)	0.3277 (6)	0.5863 (6)
C33	0.5927 (2)	0.2505 (6)	0.5350 (7)
C34	0.5678 (3)	0.2227 (4)	0.4337 (7)
C35	0.4586 (2)	0.3185 (4)	0.1983 (5)
C36	0.4096 (3)	0.3344 (5)	0.2168 (5)
C37	0.3798 (3)	0.4117 (7)	0.1774 (7)
C38	0.3985 (4)	0.4775 (6)	0.1132 (7)
C39	0.4443 (4)	0.4650 (5)	0.0907 (7)
C40	0.4738 (3)	0.3878 (5)	0.1327 (6)
C41	0.5362 (2)	0.2044 (4)	0.1791 (5)
C42	0.5808 (3)	0.2526 (5)	0.1849 (6)
C43	0.6148 (3)	0.2315 (6)	0.1169 (7)
C44	0.6051 (3)	0.1619 (5)	0.0420 (7)
C45	0.5615 (3)	0.1125 (5)	0.0335 (6)
C46	0.5278 (2)	0.1327 (4)	0.1007 (6)
C47	0.4622 (2)	0.1314 (4)	0.2634 (5)
C48	0.4787 (2)	0.0611 (4)	0.3406 (5)
C49	0.4544 (3)	−0.0270 (4)	0.3390 (6)
C50	0.4117 (3)	−0.0464 (5)	0.2630 (7)
C51	0.3944 (2)	0.0196 (6)	0.1869 (6)
C52	0.4190 (3)	0.1088 (5)	0.1876 (6)
B	0.4946 (2)	0.2309 (5)	0.2548 (6)

[a] The esd's in parentheses for this and all subsequent tables refer to the least significant figures.

---

[22] This automatic reflection-indexing algorithm is based upon Jacobson's procedure: Jacobson, R. A. *J. Appl. Crystallogr.* **1976**, *9*, 115.

[23] The peak-centering algorithm is similar to that described by Busing: Busing, W. R. In *Crystallographic Computing*; Ahmed, F. R., Ed.; Munksgaard: Copenhagen, 1970; p 319. The ω, χ, and 2θ angles were optimized with respect to the Kα_1 peak (λ = 0.709 26 Å).

[24] Declerq, J. P.; Germain, D.; Main, P.; Woolfson, M. M. *Acta Crystallogr., Sect. A* **1973**, *A29*, 231.

[25] Calabrese, J. C. Ph.D. Dissertation, University of Wisconsin—Madison, 1971.

Table III. Selected Interatomic Distances (Å) and Bond Angles (deg) in $[Cp^*_2Zr(CH_2SiMe_3)(THF)][B(C_6H_5)_4]$[a,b]

A. Interatomic Distances (Å)

Zr–O	2.243 (3)	Zr–C1	2.238 (6)
Zr–Cp(1)[a]	2.257 (7)	Zr–Cp(2)	2.255 (7)
Si–C1	1.904 (6)	Si–C2	1.854 (6)
Si–C3	1.853 (8)	Si–C4	1.871 (7)
O–C5	1.472 (8)	O–C8	1.471 (8)
C5–C6	1.479 (9)	C8–C7	1.487 (10)
C6–C7	1.419 (14)		

range of 10 Zr–C distances (Cp* rings): 2.522 (6)–2.581 (5)
range of 10 C–C distances (Cp* rings): 1.388 (9)–1.416 (13)
range of 10 C–C(methyl) distances (Cp* rings): 1.489 (11)–1.524 (12)
range of 4 B–C distances (BPh_4^- anion): 1.627 (9)–1.654 (9)
range of 24 C–C distances (BPh_4^- anion): 1.332 (15)–1.414 (8)

B. Bond Angles (deg)

C1–Zr–O	91.7 (2)	Cp(1)–Zr–Cp(2)	135.2 (3)
Zr–C1–Si	149.9 (3)	C5–O–C8	106.3 (4)
Zr–O–C5	128.0 (3)	Zr–O–C8	125.7 (4)
O–C5–C6	107.3 (6)	O–C8–C7	108.3 (6)
C5–C6–C7	109.5 (6)	C8–C7–C6	106.4 (7)
C1–Si–C2	116.3 (3)	C2–Si–C3	106.3 (3)
C1–Si–C3	110.7 (3)	C2–Si–C4	106.2 (3)
C1–Si–C4	111.3 (3)	C3–Si–C4	105.3 (3)

range of 10 C–C–C angles (Cp* rings): 107.4 (7)–108.7 (7)
range of 20 C–C–C(methyl) angles (Cp* rings): 122.0 (7)–128.0 (7)
range of 6 C–B–C angles (BPh_4^- anion): 106.2 (5)–112.3 (5)
range of 8 B–C–C angles (BPh_4^- anion): 121.8 (5)–124.0 (5)
range of 24 C–C–C angles (BPh_4^- anion): 112.9 (6)–124.4 (7)

[a] Cp(*n*) denotes the centroid of a cyclopentadienyl ring. Cp(1) and Cp(2) contain carbon atoms C9–C13 and C14–C18, respectively. [b] The esd's for the interatomic distances and bond angles were calculated from the standard errors of the fractional coordinates of the corresponding atomic positions.

of the positional and anisotropic thermal parameters for the 56 non-hydrogen atoms with isotropic contributions for 65 of the 69 hydrogen atoms led to final discrepancy indices of $R(F_o) = 0.052$, $R(F_o^2) = 0.062$, $R_w(F_o^2) = 0.096$, and $\sigma_1 = 1.81$ for 3608 reflections with $F_o^2 > 3\sigma(F_o^2)$. A final difference map did not reveal any regions of significant residual electron density.

The positional parameters for the refined non-hydrogen atoms are given in Table II. Selected interatomic distances and bond angles and their esd's are given in Table III. Tables of thermal parameters, the equations of pertinent least-squares planes and their dihedral angles, and tables of observed and calculated structure factors are available as supplementary material.[31]

Results and Discussion

Protonation of 1-Sila-3-metallacyclobutanes. Protonation of a methylene group of a 1-sila-3-metallacyclobutane ring with a bulky trialkylammonium cation provides a general synthetic method for the preparation of group 4 metallocene trimethylsilylmethyl cations. In THF solvent, the newly created coordination site is occupied by the oxygen atom of a coordinated THF molecule (eq 2).

$$L_n\overline{M(CH_2SiMe_2C}H_2) + [NR_3H][BPh_4] \xrightarrow{THF} [L_nM(CH_2SiMe_3)(THF)][BPh_4] + NR_3 \qquad (2)$$

The ease with which the cations can be isolated as analytically pure materials is dependent on the choice of the ancillary cyclopentadienyl ligand. When the protonation of $Cp_2\overline{M(CH_2SiMe_2C}H_2)$ (M = Ti, Zr) with $[NEt_3H][BPh_4]$ is performed at 25 °C, the resultant salts, **1** and **2** (eq 3), where initially contaminated with a small amount

$$Cp_2\overline{M(CH_2SiMe_2C}H_2) + [NEt_3H][BPh_4] \xrightarrow{THF} [Cp_2M(CH_2SiMe_3)(THF)][BPh_4] + NEt_3 \qquad (3)$$
$$M = Ti (\mathbf{1}), Zr (\mathbf{2})$$

of unreacted ammonium salt. This impurity is easily removed by washing the product with cold CH_2Cl_2. However, some of the desired product also dissolves, thereby resulting in a lower isolated yield. For the corresponding *ansa*-metallocene compounds $[SiMe_2(C_5H_4)_2]\overline{M(CH_2SiMe_2C}H_2)$ (M = Ti, Zr), structural studies[12] have shown that the introduction of the $SiMe_2$ bridge results in a 7–10° increase in the dihedral angle between the cyclopentadienyl rings and does not significantly modify the structural parameters within the 1-sila-3-metallacyclobutane ring. Opening the wedge with this modification enhances the ability of the NEt_3H^+ cation to transfer its proton to a more accessible methylene carbon center. As a consequence, the *ansa*-metallocene cations **3** and **4** are isolated from reaction 4 in high yields without significant

$$[SiMe_2(C_5H_4)_2]\overline{M(CH_2SiMe_2C}H_2) + [NEt_3H][BPh_4] \xrightarrow{THF} \{[SiMe_2(C_5H_4)_2]M(CH_2SiMe_3)(THF)\}[BPh_4] + NEt_3$$
$$M = Ti (\mathbf{3}), Zr (\mathbf{4}) \qquad (4)$$

contamination from unreacted $[NEt_3H][BPh_4]$. Any excess metallacycle and triethylamine is readily removed by washing the product with small portions of pentane.

The salt that proved to be the most difficult to isolate is $[Cp^*_2Zr(CH_2SiMe_3)(THF)][BPh_4]$ (**5**). The purification of this salt is complicated by the lability of the coordinated THF ligand, which is removed incrementally during successive washings of **5** with toluene. The subsequent formation of the "THF-free" cation $[Cp^*_2Zr(CH_2SiMe_3)]^+$, as tentatively identified by ^1H NMR measurements, is followed by an intramolecular C–H activation process that results in the elimination of $SiMe_4$ (eq 1). Despite the use of a 15–20% excess of the metallacycle in eq 5, NMR and

$$Cp^*_2\overline{Zr(CH_2SiMe_2C}H_2) + [NEt_3H][BPh_4] \xrightarrow{THF} \underset{\mathbf{5}}{[Cp^*_2Zr(CH_2SiMe_3)(THF)][BPh_4]} + NEt_3 \qquad (5)$$

elemental analyses of **5** indicate the presence of a detectable amount of $[NEt_3H][BPh_4]$. This difficulty may in part be a consequence of the steric congestion introduced by the Cp* ligands, which may hinder the approach of NEt_3H^+ during the protonation of $Cp^*_2\overline{Zr(CH_2SiMe_2C}H_2)$. Even refluxing the reactants at 60 °C for several hours is not sufficient to ensure complete consumption of the ammonium salt. Efforts to remove this impurity with cold CH_2Cl_2 washes are thwarted by the greater solubility and reactivity displayed by **5** (by comparison to **1**–**4**) toward this solvent.

---

(26) The least-squares refinement[27] of the X-ray diffraction data was based upon the minimization of $\sum w_i|F_o^2 - S^2F_c^2|^2$, where w_i is the individual weighting factor and S is the scale factor. The discrepancy indices were calculated from the expressions $R(F_o) = \sum||F_o| - |F_c||/\sum|F_o|$, $R(F_o^2) = \sum|F_o^2 - F_c^2|/\sum F_c^2$, and $R_w(F_o^2) = [\sum w_i|F_o^2 - F_c^2|^2/\sum w_iF_o^4]^{1/2}$. The standard deviation of an observation of unit weight, σ_1, equals $[\sum w_i|F_o^2 - F_c^2|/(n - p)]^{1/2}$, where n is the number of observations and p is the number of parameters varied during the last refinement cycle.

(27) The scattering factors employed in all of the structure factor calculations were those of Cromer and Mann[28] for the non-hydrogen atoms and those of Stewart et al.[29] for the hydrogen atoms with corrections included for anomalous dispersion.[30]

(28) Cromer, D. T.; Mann, J. B. *Acta Crystallogr., Sect. A* **1968**, *A24*, 231.

(29) Stewart, R. F.; Davidson, E. R.; Simpson, W. T. *J. Chem. Phys.* **1965**, *42*, 3175.

(30) Cromer, D. T.; Liberman, D. J. *J. Chem. Phys.* **1970**, *53*, 1891.

(31) The computer programs that were used for the X-ray diffraction data analysis are described in: Nicholson, G. A.; Petersen, J. L.; McCormick, B. J. *Inorg. Chem.* **1980**, *19*, 195.

The characterization of **1**–**5** in solution was accomplished by ^1H and ^{13}C NMR measurements. Although these cations readily abstract Cl from methylene chloride, the degradation of **1**–**4** in CD_2Cl_2 is sufficiently slow ($t_{1/2} \approx 1$ day) to permit accumulation of their ^1H and $^{13}C\{^1H\}$ NMR spectra. Compound **5** is sufficiently soluble in toluene-d_8 to permit measurement of its ^1H NMR spectrum. The ^1H NMR data for **1**–**5** reflect the mode of THF coordination in each cation. The resonances of the α-CH_2 and β-CH_2 protons of the coordinated THF molecule in **1**–**4** are shifted significantly upfield from those of free THF in CD_2Cl_2.[32] In contrast, the α-CH_2 and β-CH_2 proton resonances of the weakly bound THF molecule in **5** correspond closely to those observed for free THF in toluene-d_8.[32] This variation is a consequence of the mode of THF coordination, with it being either oriented "perpendicular" to the equatorial plane of the metallocene wedge as in $[Cp_2ZrMe(THF)][BPh_4]$[33] or "parallel" to it as in $[Cp^*_2TiMe(THF)][BPh_4]$.[7] In the former arrangement, the noticeable upfield shift of the α-CH_2 protons results from the shielding provided by the π-electron clouds of the nearby cyclopentadienyl rings. As expected, the resonances for the more distant β-CH_2 protons are shielded to a lesser extent.

The Ti–CH_2 proton resonances at δ 3.41 (**1**) and 3.39 (**3**) are shifted by ca. 1.2 ppm downfield from their corresponding values of δ 2.17 and 2.20 in the neutral compounds $Cp_2Ti(CH_2SiMe_3)Cl$[34] and $[SiMe_2(C_5H_4)_2]Ti(CH_2SiMe_3)Cl$,[34] respectively. The Zr–CH_2 resonances at δ 1.67 (**2**) and 1.52 (**4**) are shifted downfield by ca. 0.7 ppm from their values of δ 0.93 and 0.88 in $Cp_2Zr(CH_2SiMe_3)Cl$[34] and $[SiMe_2(C_5H_4)_2]Zr(CH_2SiMe_3)Cl$,[34] respectively. The corresponding Zr–CH_2 proton resonance of **5** is also found downfield at δ 1.76. The positive charge of these cations, by drawing electron density toward the metal from the methylene groups, leads to a deshielding of the methylene proton nuclei and a downfield shift of their NMR resonance.

The protonation of $Cp^*_2\overline{Zr(CH_2SiMe_2CH_2)}$ with the soluble ammonium salt $[N(n\text{-butyl})_3H][BPh_4]$ proceeds at 25 °C in toluene with the formation of a highly air-sensitive orange precipitate. The composition of this material (**6**) on the basis of elemental analyses and spectroscopic data is compatible with that of the zwitterion $Cp^*_2Zr(+)\text{-}(m\text{-}C_6H_4)\text{-}B(-)Ph_3$, originally isolated by Turner and coworkers[21] from the reaction of $Cp^*_2ZrMe_2$ with $[N(n\text{-butyl})_3H][BPh_4]$. Compound **6** is presumably formed by a two-step process (eq 6).

$$\begin{aligned} &Cp^*_2\overline{Zr(CH_2SiMe_2CH_2)} + \\ &\qquad [N(n\text{-butyl})_3H][BPh_4] \xrightarrow[25\ ^\circ C]{toluene} \\ &\qquad [Cp^*_2Zr(CH_2SiMe_3)][BPh_4] \xrightarrow{-SiMe_4} \\ &\qquad\qquad Cp^*_2Zr(+)\text{-}(m\text{-}C_6H_4)\text{-}B(-)Ph_3 \quad (6) \\ &\qquad\qquad\qquad \mathbf{6} \end{aligned}$$

Protonation of $Cp^*_2\overline{Zr(CH_2SiMe_2CH_2)}$ initially affords the cation $[Cp^*_2Zr(CH_2SiMe_3)]^+$. In the *absence* of a coordinating substrate, such as THF, this cation is sufficiently reactive to activate a meta C–H bond of BPh_4^-, resulting in the loss of $SiMe_4$ and the precipitation of **6**. The apparent kinetic preference of the intermediate $[Cp^*_2Zr(CH_2SiMe_3)]^+$ cation toward this intermolecular C–H activation process over the potentially competitive, intramolecular activation of a C–H bond of a Cp* ligand (see (1)) is probably a consequence of the greater concentration of BPh_4^- under these reaction conditions.

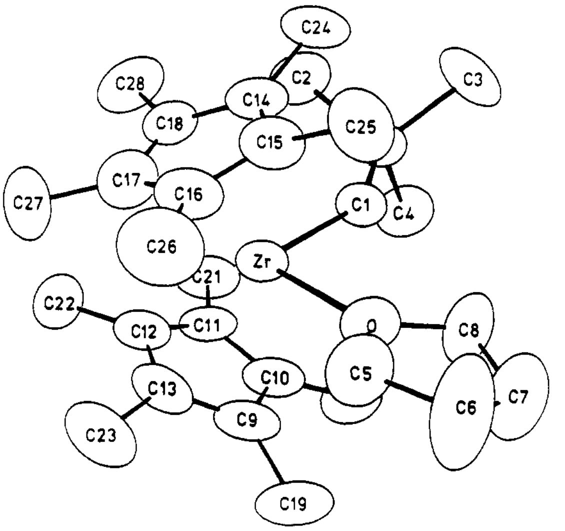

Figure 1. Perspective view of the molecular structure of $[Cp^*_2Zr(CH_2SiMe_3)(THF)]^+$ with the atom-numbering scheme. The thermal ellipsoids have been scaled to enclose 50% probability, and the hydrogen atoms have been removed for the purpose of clarity.

Description of the Molecular Structure of $[Cp^*_2Zr(CH_2SiMe_3)(THF)][BPh_4]$. An X-ray structural analysis of $[Cp^*_2Zr(CH_2SiMe_3)(THF)][BPh_4]$ was undertaken to establish the molecular structure of the cation and determine the mode of THF coordination. This compound crystallizes in a monoclinic crystal lattice of $P2_1/a$ symmetry with four discrete cations and anions per unit cell. A perspective view of the molecular structure of $[Cp^*_2Zr(CH_2SiMe_3)(THF)]^+$ with the atom-labeling scheme is depicted in Figure 1. The coordination environment about the zirconium atom consists of two π-bonded Cp* rings, a (trimethylsilyl)methyl ligand, and an η^1-oxygen-bound THF ligand. The $SiMe_3$ group of the (trimethylsilyl)methyl ligand is directed away from the THF ligand in the same general manner as observed by Lappert and co-workers[35] for the neutral dialkyl complex $Cp_2Zr(CH_2SiMe_3)_2$. The Zr–C1–Si angle in $[Cp^*_2Zr(CH_2SiMe_3)(THF)]^+$ of 149.9 (3)°, which is ca. 15° larger than the corresponding angles in $Cp_2Zr(CH_2SiMe_3)_2$,[35] rules out a γ-agostic Zr⋯H(CH_3) interaction. Alternatively, the low $^1J_{C-H}$ coupling constant[36] of 100.1 Hz for the methylene carbon of **5** might suggest the possible existence of an α-agostic interaction. The rather long Zr⋯H1 and Zr⋯H2 separations[37] of 2.72 (5) and 2.57 (5) Å, respectively, are incompatible with this situation.

The THF ligand in **5** is nearly coplanar with the equatorial plane (defined by carbon C1, Zr, and O) that symmetrically bisects the wedge of the Cp^*_2Zr fragment. This

---

[32] The α-CH_2 and β-CH_2 proton NMR resonances of THF appear at δ 3.70 and 1.87 in CD_2Cl_2 and δ 3.55 and 1.46 in toluene-d_8, respectively.

[33] Jordan, R. F.; Bajgur, C. S.; Willett, R.; Scott, B. *J. Am. Chem. Soc.* **1986**, *108*, 7410.

[34] The ^1H NMR resonances observed for the methylene protons of the neutral complexes $Cp_2Ti(CH_2SiMe_3)Cl$, $Cp_2Zr(CH_2SiMe_3)Cl$, $[SiMe_2(C_5H_4)_2]Ti(CH_2SiMe_3)Cl$, and $[SiMe_2(C_5H_4)_2]Zr(CH_2SiMe_3)Cl$ were determined by monitoring the degradation of the corresponding metallocene cations in CD_2Cl_2.

[35] (a) Jeffrey, J.; Lappert, M. F.; Luong-Thi, N. T.; Webb, M.; Atwood, J. L.; Hunter, W. E. *J. Chem. Soc., Dalton Trans.* **1981**, 1593. (b) Collier, M. R.; Lappert, M. F.; Pearce, P. *J. Chem. Soc., Dalton Trans.* **1973**, 445.

[36] Jordan, R. F.; Bradley, P. K.; Baenziger, N. C.; LaPointe, R. E. *J. Am. Chem. Soc.* **1990**, *112*, 1289.

[37] The refined atomic coordinates for H1 and H2 were corrected to account for the inherent shortening observed for X-ray-determined C–H bond distances.

Table IV. Comparison of Pertinent Structural Parameters from the X-ray Structural Analyses of $[Cp_2ZrMe(THF)]^+$ and $[Cp^*_2Zr(CH_2SiMe_3)(THF)]^+$

	$[Cp_2ZrMe(THF)]^{+a}$	$[Cp^*_2Zr(CH_2SiMe_3)(THF)]^+$
Zr–O, Å	2.122 (14)	2.243 (3)
Zr–C(alkyl), Å	2.256 (10)	2.238 (6)
C(alkyl)–Zr–O, deg	97.4 (5)	91.7 (2)
Zr–Cp(c), av	2.174	2.256 (7)
acute dihedral angle between C-Zr-O and C-O-C planes, deg	77.7	13.6

[a] Reference 33.

arrangement is distinctly different from that observed by Jordan and co-workers[33] for the THF ligand in $[Cp_2ZrMe(THF)]^+$ but is analogous to that reported by Bochmann and co-workers[7] for the structure of the $[Cp^*_2TiMe(THF)]^+$ cation. In the former case, the acute dihedral angle between the C–O–C plane of the THF ligand and the C(methyl)–Zr–O plane is 77.7°, compared to a dihedral angle of 13.6° in **5**. The greater steric bulk of the Cp* ligands clearly has a significant stereoelectronic influence on the mode of THF coordination and the relative strength of the Zr–O bond.

Pertinent structural parameters for $[Cp_2ZrMe(THF)]^+$[33] and $[Cp^*_2Zr(CH_2SiMe_3)(THF)]^+$ are compared in Table IV. The structural differences associated with these two cations can be rationalized by considering the frontier orbital interactions associated with the "perpendicular" and "parallel" THF coordination modes. As a Lewis base, THF normally coordinates by using one of the two lone pairs on the oxygen atom, producing a trigonal-pyramidal arrangement of bonded atoms around the oxygen. However, the sum of the three relevant bond angles about the oxygen donor atom in $[Cp^*_2Zr(CH_2SiMe_3)(THF)]^+$ is 360.0°. Analogous trigonal-planar geometries about the oxygen atom of a η^1-coordinated THF ligand have been noted in several structurally similar metallocene complexes, including $Cp_2YbMe(THF)$[38] (358.5°), $Cp^*_2YMe(THF)$[39] (359.4°), and $Cp^*_2SmMe(THF)$[40] (360°). This structural information reflects an apparent rehybridization of the two O-donor orbitals in THF to produce a σ-donor orbital of "sp^2" character and π-donor orbital of primarily "p" character. The additional s character of the former should enhance its ability to donate to the electrophilic metal center. In these d^0 metallocene systems a vacant hybridized d orbital of a_1 symmetry[41] is also available to accept additional electron density from the other oxygen orbital via π-donation. To optimize the orbital overlap associated with this interaction, the THF must adopt a perpendicular orientation. In **5** the additional steric bulk of the Cp* ligands prevents this arrangement, thereby leading to a significant elongation of the Zr–O bond from 2.122 (14) Å in $[Cp_2ZrMe(THF)]^+$[33] to 2.243 (3) Å in $[Cp^*_2Zr(CH_2SiMe_3)(THF)]^+$. A similar absence of a π-interaction is also reflected by the corresponding Ti–O bond distance of 2.154 (6) Å in $[Cp^*_2TiMe(THF)]^+$.[7]

The Zr–C(alkyl) bond distance of 2.238 (6) Å in **5** being ca. 0.04 Å shorter than typically found in neutral zirconocene bis(hydrocarbyl) complexes (Cp_2ZrMe_2,[42] 2.278 Å (average); $Cp_2Zr(CH_2CMe_3)_2$,[35] 2.294 (8) Å; $Cp_2Zr(CH_2SiMe_3)_2$,[35] 2.280 Å (average); $Cp_2Zr(CH_2PPh_2)_2$,[43] 2.284 (8) and 2.340 (9) Å) is probably a consequence of the smaller effective covalent radius of the Zr atom in the cation. Considering the greater steric size of the Cp* versus that of the Cp ligand, it is not surprising that the average Zr–Cp*(centroid) distance of 2.256 Å in $[Cp^*_2Zr(CH_2SiMe_3)(THF)]^+$ is ca. 0.08 Å longer than the average Zr–Cp(centroid) distance of 2.174 Å in $[Cp_2ZrMe(THF)]^+$.[33] As expected, the average displacement of the methyl substituents of the Cp* ligands out of the corresponding ring planes is 0.24 Å away from the metal. The tetraphenylborate anion displays the normal tetrahedral arrangement of four planar phenyl groups around the boron atom.

Metallocene Alkyl Cations as Catalysts for Ethylene Polymerization. Reactivity studies of various neutral metallocene hydrocarbyl systems, Cp^*_2MR, where M = Lu,[44] Sc,[45] La,[46] Nd,[46] and Sm,[46] indicate that these complexes are effective catalysts for the polymerization of ethylene under mild conditions in the absence of an Al cocatalyst. The enhanced Lewis acidity introduced by the apparent availability of *two* vacant metal orbitals in these $14e^-$ species plays a key role in promoting the migratory insertion of ethylene into the corresponding M–C bond. The transfer of electron density that occurs upon coordination of C_2H_4 to a high-valent, electron-deficient metal center enhances its susceptibility to intramolecular nucleophilic attack by the alkyl ligand. Because the corresponding group 4 metallocene alkyl cations $(C_5X_5)_2MR^+$ (X = H, Me) are isoelectronic with these neutral complexes, they also are expected to exhibit a high degree of activity as ethylene polymerization catalysts. Jordan and co-workers[47] have observed that their THF-stabilized species $[Cp_2ZrR(THF)]^+$ (R = Me, CH_2Ph, Ph, H, etc.) are moderately good catalysts for either the oligomerization or polymerization of ethylene. This activity is a consequence of the lability of the THF ligand, which upon its dissociation generates Cp_2ZrR^+ in situ.

The protonation of a 1-sila-3-metallacyclobutane ring by NEt_3H^+ in THF offers an alternative way of generating highly electrophilic titanocene and zirconocene cations (**1**–**5**). Their reactivity toward ethylene was examined initially in each case by using NMR spectroscopy to monitor the uptake of ethylene. The reaction of a 10–20-fold excess of ethylene in the presence of 1 equiv of **1**–**4** proceeds (over a period of several days at room temperature) in CD_2Cl_2 with the gradual disappearance of the free ethylene proton NMR resonance at δ 5.41. The parallel appearance of a broad singlet at δ 1.27 represents an envelope of methylene proton resonances arising from multiple ethylene insertions into the M–C bond of these cations. As the polymerization reaction proceeds, visual evidence of polymer formation is provided by the formation of a finely divided white solid, which floats on the methylene chloride solution. As the ethylene is consumed, catalyst deactivation by Cl abstraction from CD_2Cl_2 proceeds with the formation of the neutral metallocene alkyl

---

[38] Evans, W. J.; Dominguez, R.; Hanusa, T. P. *Organometallics* **1986**, *5*, 263.

[39] Den Haan, K. H.; De Boer, J. L.; Teuben, J. H.; Smetts, W. J. J.; Spek, A. L. *J. Organomet. Chem.* **1987**, *327*, 31.

[40] Evans, W. J.; Chamberlain, W. R.; Ulibarri, T. A.; Ziller, J. W. *J. Am. Chem. Soc.* **1988**, *110*, 6423.

[41] Lauher, J. W.; Hoffmann, R. *J. Am. Chem. Soc.* **1976**, *98*, 1729.

[42] Hunter, W. E.; Hrncir, D. C.; Vann Bynum, R.; Pentilla, R. A.; Atwood, J. L. *Organometallics* **1983**, *2*, 750.

[43] Schore, N. E.; Young, S. J.; Olmstead, M. M.; Hofmann, P. *Organometallics* **1983**, *2*, 1769.

[44] Watson, P. L. *J. Am. Chem. Soc.* **1982**, *104*, 337.

[45] (a) Thompson, M. E.; Bercaw, J. E. *Pure Appl. Chem.* **1984**, *56*, 1. (b) Burger, B. J.; Thompson, M. E.; Cotter, W. D.; Bercaw, J. E. *J. Am. Chem. Soc.* **1990**, *112*, 1566.

[46] Jeske, G.; Lauke, H.; Mauermann, H.; Swepston, P. N.; Schumann, H.; Marks, T. J. *J. Am. Chem. Soc.* **1985**, *107*, 8091.

[47] Jordan, R. F.; La Pointe, R. E.; Bradley, P. K.; Baenziger, N. *Organometallics* **1989**, *8*, 2892 and references cited therein.

chloride and the appearance of free THF.

The absence of THF significantly enhances the catalytic activity of these metallocene–alkyl cations. Small-scale reactions were carried out in sealed tubes containing equivalent amounts of the appropriate metallacycle and trialkylammonium salt, a ca. 100-fold excess of ethylene, and several milliliters of solvent. To facilitate sample preparation, the volatile components were added via vacuum transfer and kept frozen until the reaction tube was sealed. The reagents were placed in an ice bath and then shaken upon thawing of the solvent. A qualitative indication of the catalytic activity was provided by monitoring visually the rate of solid accumulation within the reaction tube.

These small-scale polymerization reactions indicate that the catalytic activity displayed by these reaction mixtures depends on the solvent, the metal, and the type of cyclopentadienyl ligand. The species generated upon protonation of each metallacyclic precursor exhibits significantly higher activity in CH_2Cl_2 than in toluene. The only material that readily polymerizes ethylene in toluene is the zwitterion $Cp^*{}_2Zr(+)$-(*m*-C_6H_4)-$B(-)Ph_3$ (**6**). The polymerization reaction in this case is complete after several minutes. The white insoluble product was identified by comparing its IR spectrum, density, and melting point with those of polyethylene. The IR spectrum obtained with a KBr pellet contains two bands at 2916 and 2870 cm^{-1} characteristic of methylene C–H stretches, two bands at 1470 and 1465 cm^{-1} associated with C–H bends, and absorbances at 728 and 718 cm^{-1} corresponding to methylene rocking motions. These peak locations are consistent with those at 2920, 2880, 1470, 1465, 1463, 730, and 721 cm^{-1}, reported by Aggarwal and Sweetings,[48] for polyethylene. The measured density of 0.94 g/mL, as determined by the flotation method with a CH_2Cl_2/toluene solvent mixture, compares favorably with the range of 0.94–0.965 g/mL for high-density polyethylene (HDPE).[49] Heating of a sample of the polymer in a capillary tube proceeds with a visual softening of the material at ca. 110 °C followed by melting within the temperature range of 134–137 °C. This behavior is also indicative of HDPE,[49] which exhibits a Vicat softening point at 112 °C and melts at 135 °C. The only other reaction system that shows catalytic activity in toluene is the species generated upon protonolysis of $Cp^*{}_2Zr(CH_2SiMe_2CH_2)$ by $[N(n\text{-butyl})_3H][BPh_4]$. In this case, polymer formation occurs slowly over a period of several weeks.

Similar experiments surprisingly indicate that **5** does not readily polymerize ethylene in toluene. This lack of activity may be a consequence of the large Zr–C–Si bond angle, which prohibits any significant assistance from an α-H agostic interaction[50] in stabilizing the transition state associated with the migratory insertion of ethylene into the Zr–C bond. By comparison, Teuben and co-workers[6] have reported that $[Cp^*{}_2MMe(THT)][BPh_4]$ (M = Zr, Hf) are active catalysts for the polymerization of ethylene and the oligomerization of propylene in polar solvents, such as *N,N*-dimethylaniline. Although the THT ligand of $[Cp^*{}_2MMe(THT)]^+$ and the THF ligand of **5** are labile, the resultant "base-free" cations apparently differ in their relative kinetic preference toward olefin insertion into the M–C bond versus intramolecular activation of a C–H bond of the Cp* ligand.

The catalytic species formed by protonation of $Cp_2M(CH_2SiMe_2CH_2)$, $[SiMe_2(C_5H_4)_2]M(CH_2SiMe_2CH_2)$, and $Cp^*{}_2Zr(CH_2SiMe_2CH_2)$ in CH_2Cl_2 differ significantly in the rate of polyethylene formation. The polymerization reactions initiated by treating $Cp_2Zr(CH_2SiMe_2CH_2)$ or $[SiMe_2(C_5H_4)_2]Zr(CH_2SiMe_2CH_2)$ with $[NEt_3H][BPh_4]$ are essentially complete once the frozen contents of the reaction tube are warmed and shaken at 0 °C. For the corresponding titanacyclic precursors $Cp_2Ti(CH_2SiMe_2CH_2)$ and $[SiMe_2(C_5H_4)_2]Ti(CH_2SiMe_2CH_2)$, polymer formation does not occur until the respective reaction mixture is warmed to room temperature. The apparent induction period probably reflects a slower rate for the formation of these Ti cations. The subsequent ethylene polymerization reaction proceeds to completion within 1 min. Finally, for the permethylated cyclopentadienyl precursor $Cp^*{}_2Zr(CH_2SiMe_2CH_2)$, the corresponding polymerization reaction requires over 1 week to finish. This lower activity is most likely due to a combination of factors, including the greater electron-donating character of the Cp* ligands and the availability of a competitive intramolecular C–H activation process involving Cp*. The polyethylene samples isolated from these polymerization reactions performed in CH_2Cl_2 exhibit densities ranging from 0.90 to 0.94 g/cm^3 and melting points varying from 121 to 132 °C.

Concluding Remarks. Protonation of a 1-sila-3-metallacyclobutane ring with a trialkylammonium ion provides a convenient route for converting 1-sila-3-metallacyclobutane complexes of Ti and Zr to the corresponding (trimethylsilyl)methyl-substituted metal alkyl cations. In THF, the coordination site produced during this ring-opening reaction is occupied by the oxygen donor atom of THF. By control of the orientation of the coordinated THF molecule, the steric demands of the ancillary cyclopentadienyl rings exhibit a significant stereoelectronic influence on the relative strength of the Zr–O bonds in $[Cp_2ZrMe(THF)]^+$[33] and $[Cp^*{}_2Zr(CH_2SiMe_3)]^+$. Solution NMR and structural data obtained for **5** similarly indicate that the THF ligand is weakly bound to Zr. Efforts to isolate the THF-free cation $[Cp^*{}_2Zr(CH_2SiMe_3)]^+$, however, are hindered by its ability to participate in the intramolecular and intermolecular C–H activation processes (1) and (6), respectively. The catalytic activity displayed by these electrophilic species toward the polymerization of ethylene is highly variable. Although HDPE is produced under mild conditions in the absence of an Al cocatalyst, the relative rate of polymer formation depends on the solvent, the metal, and the type of cyclopentadienyl ligand employed. Current efforts are being directed at improving the solubility of these cations in noncoordinating, halogen-free solvents and modifying their Lewis acidity.

Acknowledgment. Support for this research was provided by the donors of the Petroleum Research Fund, administered by the American Chemical Society. Computer time for the X-ray structural analysis was provided by the West Virginia Network for Educational Telecomputing. The research assistantship to D.M.A. was made possible through support provided by the West Virginia Energy and Water Research Center.

Supplementary Material Available: Tables of thermal parameters, H atom coordinates, and pertinent least-squares planes for **5** (8 pages); a listing of observed and calculated structure factors for **5** (13 pages).

---

[48] Aggarwal, S. L.; Sweeting, O. J. *Chem. Rev.* **1957**, *57*, 665.

[49] Wilkinson, G.; Stone, F. G. A.; Abel, E. W. *Comprehensive Organometallic Chemistry*; Pergamon Press: New York, 1982; Vol. 3, p 475.

[50] (a) Krauledat, H.; Brintzinger, H. H. *Angew. Chem., Int. Ed. Engl.* **1990**, *29*, 1412. (b) Piers, W. E.; Bercaw, J. E. *J. Am. Chem. Soc.* **1990**, *112*, 9406.